EuCARD-2

Enhanced European Coordination for Accelerator Research & Development

Conference/Workshop Paper

Simulation of electromagnetic scattering through the E-XFEL third harmonic cavity module

Joshi, N.Y (Manchester University and Cockcroft Institute) *et al*

13 May 2016

SIMULATION OF ELECTROMAGNETIC SCATTERING THROUGH THE E-XFEL THIRD HARMONIC CAVITY MODULE

N. Y. Joshi[†ᴛ*], R. M. Jones[†ᴛ], L. Shiliang[†‡ᴛ], N. Baboi[‡]

[†]School of Physics and Astronomy, The University of Manchester, Manchester, U.K.

[ᴛ]The Cockcroft Institute of Accelerator Science and Technology, Daresbury, U.K.

[‡]Deutsches Elektronen-Synchrotron, Hamburg, Germany

Abstract

The European XFEL (E-XFEL) is being fabricated in Hamburg to serve as an X-ray Free Electron Laser light source. The electron beam will be accelerated through linacs consisting of 1.3 GHz superconducting cavities along a length of 2.1 km. In addition, third harmonic cavities will improve the quality of the beam by linearising the field profile and hence reducing the energy spread. There are eight 3.9 GHz cavities within a single module AH1 of E-XFEL. The beam-excited electromagnetic (EM) field in these cavities can be decomposed into a series of eigenmodes. These modes are, in general, not cut-off between one cavity and the next, as they are able to couple to each other throughout the module. Here for the first time, we evaluate components of the scattering matrix for module AH1. This is a computationally expensive system, and hence we employ a Generalized Scattering Matrix (GSM) technique to allow rapid computation with reduced memory requirements. Verification is provided on reduced structures, which are compared to finite element mesh-based codes. The mode spectrum for the dipole bands of interest in an eight-cavity chain have been calculated and external Q factors for the modes are derived.

INTRODUCTION

The AH1 module [1, 2] in E-XFEL [3] contains a chain of eight superconducting (SC) cavities operating at 3.9 GHz, connected by the beam pipes and bellows. Introducing a charged particle beam into a cavity results in an EM field being excited. This field can be decomposed into a series of multi-poles -both along the axis of the cavity and transverse to it. The beam-excited longitudinal wakefield gives rise to an energy spread along the beam. The transverse component dilutes the beam emittance and can give rise to a beam break up (BBU) instability [4]. Here we focus on the latter component.

The transverse component of the beam-excited wakefield can be decomposed into a series of multi-poles. Provided the beam is close to the axis of the cavity however, the dipole part will dominate, and consequently we restrict our study to this component of the multi-pole [4]. This dipole field is also decomposed into a series of modes, which are in principle infinite. However, we confine our study to those having the largest impact on the transverse momentum of the beam. These higher order dipole modes can be utilised to determine the beam position, and can also be used to align the beam

on the cavity axis. Moving the beam to the electrical centre minimises excitation of these damaging HOMs. We also use these HOMs to measure the misalignment of cavities. The frequencies of these HOMs in the third harmonic cavity (3HC) are above the beam pipe cut-off frequency and consequently the majority of the modes in the cavities couple to cavities throughout the chain in the module. This is in contradistinction to those in the 1.3 GHz cavities, which mainly consist of modes trapped within each individual cavity. Thus in these 3.9 GHz cavities it is necessary to model the complete chain as they essentially behave as one cavity *en masse*.

As the majority of the dipole modes propagate throughout the AH1 module, it is effectively a 72-cell cavity. We focus on calculating the S-matrix of this module. Modelling this accurately would require the capability of supercomputers equipped with appropriately large memory and computing speed. To obviate these requirements we employ a well-established technique of electromagnetics known as the GSM [5], which essentially entails breaking up the structure under consideration into small blocks, which are accurately computed, and then the whole set of blocks is cascaded together to evaluate the overall S-matrix. Shinton *et al.* [6] previously applied a similar technique for cavities in the FLASH modules. We provide some details on an extension of this technique in this work to a module in E-XFEL.

The next section concerns an application of GSM to a single 9-cell third harmonic cavity. The section thereafter considers the S-matrix for module AH1, and also the external Q factors of the modes with respect to the HOM couplers. The study concludes with some final remarks.

GSM APPLIED TO A SINGLE CAVITY

Here we apply the GSM technique to a 9-cell third harmonic cavity. This method allows rapid EM field calculations and S matrices to be obtained. The S-matrix of a single section is defined in the usual manner [7] in terms of incident waves (A_1, A_2) scattered off a discontinuity (B_1, B_2) as,

$$\begin{pmatrix} B_1 \\ B_2 \end{pmatrix} = \begin{pmatrix} S_{11} & S_{12} \\ S_{21} & S_{22} \end{pmatrix} \begin{pmatrix} A_1 \\ A_2 \end{pmatrix} \tag{1}$$

We cascade two junctions [5] (L for left matrix and R for right matrix) to obtain the overall R to L S-matrix as,

$$S_{11}^{LR} = S_{11}^L + S_{12}^L \left[I - S_{11}^R S_{22}^L \right]^{-1} S_{11}^R S_{21}^L, \tag{2}$$

$$S_{12}^{LR} = S_{12}^L \left[I - S_{11}^R S_{22}^L \right]^{-1} S_{12}^R, \tag{3}$$

$$S_{21}^{LR} = S_{21}^{R} \left[I - S_{22}^{L} S_{11}^{R} \right]^{-1} S_{21}^{L} \qquad (4)$$

$$S_{22}^{LR} = S_{22}^{R} + S_{21}^{R} \left[I - S_{22}^{L} S_{11}^{R} \right]^{-1} S_{22}^{L} S_{12}^{R}. \qquad (5)$$

We repeat this process to obtain the S-matrix of a complete structure. In order to gain same confidence in the accuracy of this method, we first apply it to single 9-cell third harmonic cavity and compare the results with a full structure using HFSS [8] with no concatenation used. A code has been developed in the Python programming language to implement the GSM method. The code reads the S-matrices exported from the finite element code HFSS. This code is flexible enough to import data from other codes such as CST [9].

Each 3H cavity has nine elliptical cells, a fundamental power (F) coupler, and two HOM (H1, H2) couplers. A single 9-cell cavity and the corresponding unit blocks used for GSM are shown in Fig. 1. The full structure was divided at the equator planes of the cells to improve accuracy of the cascading process, in order to maximise the number of propagating modes at any frequency. All cylindrical ports at the equator and beam pipe ends were simulated retaining 25 modes, while five modes were used at F and HOM coaxial couplers. Intrinsic wall losses, minimal in SC cavities, were not considered, and no symmetry planes were imposed.

(a) Unit blocks used to reconstruct a single cavity
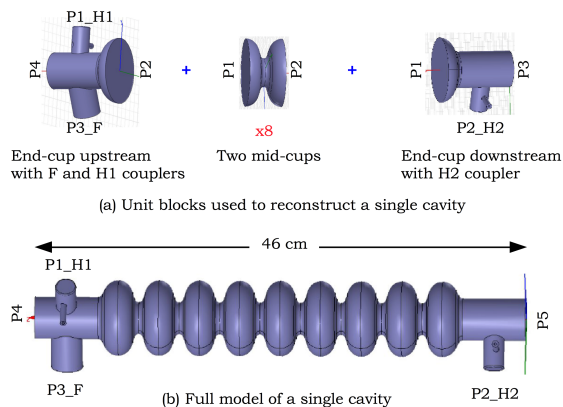

(b) Full model of a single cavity

Figure 1: CAD model of a single 9-cell third harmonic cavity drawn with HFSS. Constituent components used in the GSM simulations are shown in (a) along with the full cavity in (b).

We focused this test case on the first dipole band which is confined to the region 4.2 GHz to 5.2 GHz. A non-interpolating discrete frequency step of 500 kHz was chosen. In all simulations we used a standard high performance desktop computer equipped with 128 Gb of RAM and 48 processor cores for the HFSS simulations.The total mesh size and simulation time for each model are listed in Table 1.

The S-matrix from the unit block of two mid-cups was cascaded eight times. The cascading of the S-matrices, for 2000 frequency steps, on a standard desktop computer (with 4 cores and 16 GB RAM) took under 2 minutes. A comparison of the S-matrices for both the full structure (simulated

Table 1: Mesh Size and Simulation Time for the Unit Blocks and Full Model

Model	Simulation Parameters	
	Mesh (tets)	Time (Hours)
End-cup upstream	73019	41
Two mid-cups	31320	28
End-cup downstream	60958	33
Full cavity structure	234175	204

directly with HFSS) and the GSM method is illustrated in Fig. 2. Good agreement is obtained for both S_{21} and S_{11}. The worst case discrepancy is no more than 2%. We note that in this situation GSM is only a factor of two faster than a direct simulation with HFSS. However, when simulating multiple cavities GSM is required as the memory requirements would be impractical. Indeed, AH1 consists of 8 cavities and a direct finite element evaluation of the S matrix would necessitate the capability of a supercomputer. In the next section we simulate the S matrix for AH1 using GSM.
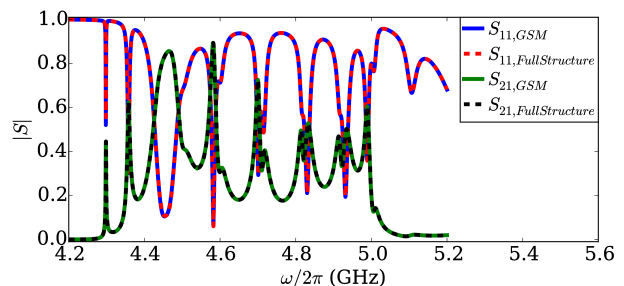

Figure 2: Comparison of S-parameters obtained through GSM and EM simulation of a single XFEL 3H cavity.

S-MATRIX OF THE AH1 MODULE

Module AH1 is designed such that the couplers on concurrent cavities are rotated by 180 degrees with respect to each other. In the GSM method this requires us to simulate the end blocks separately. These matrices for the first two cavities were then used as the unit blocks to further calculate the complete eight cavity chain. To reduce simulation time, a plane cylindrical waveguide connects the cavities, instead of the bellows. We neglect bellows at this stage as they are a small perturbation on the waveguide wall and we do not anticipate them modifying the results appreciably. An equivalent cavity chain model and the 26 ports dynamically generated during the GSM calculation are shown in Fig. 3.

The transmission parameters, from HOM-1 port of cavity-1 (C1H1) to the HOM-2 ports on Cavity-2,4,6 and 8, are displayed in Fig. 4. The frequencies in our simulation ranged from 4.2 GHz to 9.1 GHz and this ensures five dipole bands are covered. Throughput this region, illustrated in Fig. 4, it is clear that most of the signal is well transmitted (with a minimum loss of 25 dB), hence very few of the modes are trapped within cavities.
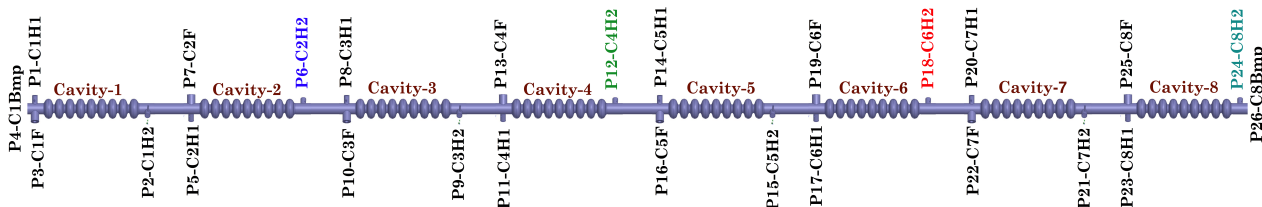
05 Beam Dynamics and Electromagnetic Fields

D03 Calculations of EM Fields - Theory and Code Developments

Figure 3: Port allocation along the eight-cavity chain.
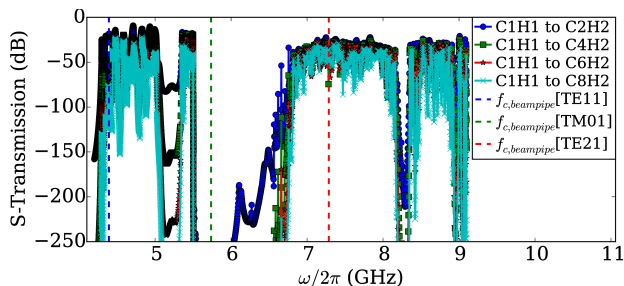
Figure 4: Amplitude of transmission coefficient along cavity chain.

Figure 5: Fitting Lorentzian functions to S_{21} curves.

Figure 6: Q_l as a function of resonant frequency.

To verify that our computations are numerically correct, we calculated the sum over all propagating modes of $|S_{11}|^2 + |S_{21}|^2$. This was found to be unity, throughout apart from one resonant point in which is deviated from unity by 0.025. We also note that this conservation condition does not provide validation as to whether or not a sufficient number of modes have been used. This provided motivation for studying the S matrix of a single cavity (as outlined in the previous section).
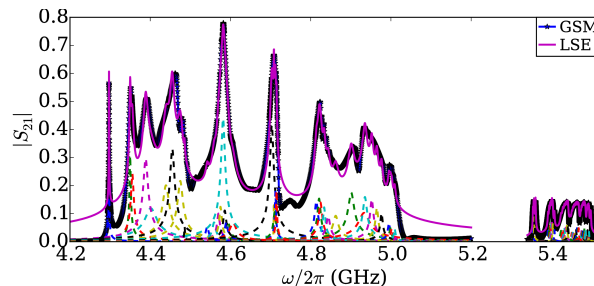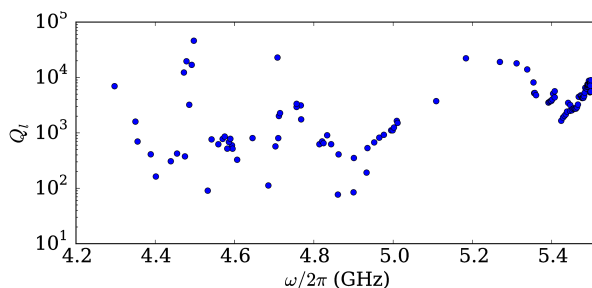
We also evaluated the loaded quality factors Q_l of these modes, viewed from the HOM coupler ports. To this end we employed a circuit model and evaluated both S_{21} and S_{11} in terms of Q_l [7]. Here we confine ourselves to an analysis of the quality factor dependence of the transmission parameter:

$$|S_{21}| \approx \frac{|\hat{S_{21}}|}{\sqrt{1 + (2Q_l\Delta)^2}}, \qquad (6)$$

where $|\hat{S_{21}}|$ is the magnitude of the transmission coefficient at resonant frequency $\omega_r/2\pi$, $\Delta = (\omega - \omega_r)/\omega_r$ and the drive frequency is $\omega/2\pi$.

We focused on the first two dipole bands and made a least square error (LSE) fit to the characteristic resonances. This is also shown in Fig. 5. We note that fitting individual modes alone was not sufficiently accurate as the tails of each resonance modified the transmission -and hence we simultaneously fitted all resonances within each band. We fitted 55 within the first band and 64 within the second band; 4.2 to 5.2 GHz and 5.2 GHz to 5.5 GHz, respectively.

These Q factors as a function of the mode resonances are displayed in Fig. 6. All are below 10^5, which is indicative of a well-damped cavity.

FINAL REMARKS

The GSM technique has been applied to calculate the S-matrix of both a single 9-cell third harmonic cavity, and 8 of these cavities in a chain. The former was compared to that simulated with the HFSS code, and good agreement was obtained. The latter, corresponded to that present in the AH1 module at the E-XFEL. Here we found a plethora of modes, but all with an external quality factors in the range 10^2 to less than 10^5 -indicating good wakefield suppression. As the modes are closely spaced, it represents a challenge to implement HOM-based BPMs based on these frequencies. Finally we note that, in order to expedite simulations we used straight cylindrical connections between cavities, rather than the bellows present in AH1. Further work is in progress on assessing the affect of including these bellows in simulations.

ACKNOWLEDGEMENTS

REFERENCES

[1] P. Pierini *et al.*, in *Proc. SRF2013*, pp. 100-102.

[2] N. Solyak *et al.*, in *Proc. PAC'03*, pp. 1213-1215.

[3] M. Altarelli *et al.*, DESY, Hamburg, Germany, Rep. DESY 2006-097, 2006.

[4] R. M. Jones, *Phys. Rev. ST Accel. Beams*, vol. 12, no. 10, p. 104801, Oct 2009.

[5] T. Itoh (Ed.), *Numerical techniques for microwave and millimeter-wave passive structures*. Hoboken, NJ, USA: John Wiley & Sons, 1989.

[6] I. R. R. Shinton *et al.*, in *Proc. IPAC'10*, pp. 3007-3009.

[7] D. Z. M. Pozar, *Microwave Engineering*. Hoboken, NJ, USA: John Wiley & Sons, 2011.

[8] Ansys HFSS, `http://www.ansys.com`

[9] CST, `https://www.cst.com/Products/CSTMWS`